Intensive Care Med (1998) 24: 829–836

EXPERIMENTAL

I. Frerichs
G. Hahn
T. Schröder
G. Hellige

Electrical impedance tomography in monitoring experimental lung injury

Received: 22 December 1997
Accepted: 7 April 1998

Supported by the Deutsche Forschungsgemeinschaft, SFB 330, Göttingen and the German Aerospace Center, Bonn, Germany

I. Frerichs (✉) · G. Hahn ·
T. Schröder · G. Hellige
Department of Anaesthesiological Research, Centre of Anaesthesiology, Emergency and Intensive Care Medicine
TL 195, University of Göttingen,
Robert-Koch-Strasse 40,
D-37075 Göttingen, Germany
Tel.: + (49)551/39—5919;
Fax: + (49)/551/39–8676

Abstract *Objective*: To apply electrical impedance tomography (EIT) and the new evaluation approach (the functional EIT) in monitoring the development of artificial lung injury.
Design: Acute experimental trial.
Setting: Operating room for animal experimental studies at a university hospital.
Subjects: Five pigs (41.3 ± 4.1 kg, mean body weight ± SD).
Interventions: The animals were anaesthetised and mechanically ventilated. Sixteen electrodes were attached on the thoracic circumference and used for electrical current injection and surface voltage measurement. Oleic acid was applied sequentially (total dose 0.05 ml/kg body weight) into the left pulmonary artery to produce selective unilateral lung injury.
Measurements and results: The presence of lung injury was documented by significant changes of $PaCO_2$ (40.1 mmHg vs control 37.1 mmHg), PaO_2 (112.3 mmHg vs 187.5 mmHg), pH (7.35 vs 7.42), mean pulmonary arterial pressure (29.2 mmHg vs 20.8 mmHg) and chest radiography. EIT detected 1) a regional decrease in mean impedance variation over the affected left lung (–41.4 % vs control) and an increase over the intact right lung (+ 20.4 % vs control) indicating reduced ventilation of the affected, and a compensatory augmented ventilation of the unaffected lung and 2) a pronounced fall in local baseline electrical impedance over the injured lung (–20.6 % vs control) with a moderate fall over the intact lung (–10.0 % vs control) indicating the development of lung oedema in the injured lung with a probable atelectasis formation in the contralateral one.
Conclusion: The development of the local impairment of pulmonary ventilation and the formation of lung oedema could be followed by EIT in an experimental model of lung injury. This technique may become a useful tool for monitoring local pulmonary ventilation in intensive care patients suffering from pulmonary disorders associated with regionally reduced ventilation, fluid accumulation and/or cell membrane changes.

Key words Lung injury · Oleic acid · Regional ventilation · Electrical impedance · Pig

Introduction

Electrical impedance tomography (EIT) is a new imaging technique providing cross-sectional images of parts of the body. The method detects the non-uniformity of the electrical properties of different tissues [1] by measuring the potential differences at the body circumference resulting from electrical current injection. Region-

al impedance data in the studied cross-section are computed using e.g. weighted back-projection [2] or error-minimizing algorithms [3] and reconstructed into an image.

A new approach in EIT data processing, designed to enhance the information content of EIT tomograms by imaging the lung function, has recently been developed in our laboratory. This technique is called functional EIT. The new functional EIT tomograms exhibit a decisively higher quality of lung images compared with simple EIT. We have checked the performance of functional EIT by local transient occlusion of peripheral airways in an experimental validation study [4]. The quantitative comparison of the results obtained by functional EIT and by reference morphological techniques revealed that 1) functional EIT identified local diminution or interruption of ventilation, 2) lung regions with reduced lung ventilation were detected in volumes as low as 20 ml and 3) the position of regions with reduced ventilation imaged by functional EIT corresponded with the morphologically established location of the affected lung areas. In an additional study in healthy human volunteers, it was examined whether the known physiological redistribution of inspired air in the lungs occurring during postural changes [5] could be determined by functional EIT. The results showed that gravity-dependent changes in regional ventilation were correctly imaged and localised by functional EIT [6], corresponding with the findings originally obtained by scintigraphic ventilation scans [5].

Considering this ability of functional EIT to follow short-term artificial [4] and physiological changes of regional ventilation [6], a new study was initiated with the intention of checking the anticipated monitoring properties of this technique in a protracted pathological disturbance of the respiratory function. An experimental model of unilateral lung injury was used and the capacity of EIT to follow the development of this lung damage over several hours was compared with concomitant measurements performed with established diagnostic tools.

Methods

Experimental set-up

Experiments were performed on five anaesthetised supine pigs (41.3 ± 4.1 kg, mean body weight ± SD) and adhered to the guidelines on animal experimentation. The protocol was approved by the state Animal Care Committee. The animals were sedated by i.m. applied azaperon (Stresnil, Janssen, Neuss, FRG) (0.25 ml/kg body weight) followed by halothane anaesthesia and paralysed by intermittent injections of pancuronium bromide (Pancuronium, Pharma, Karlsruhe, Germany). The pigs were mechanically ventilated on 50% oxygen (O_2) in nitrous oxide (N_2O) at a rate of 12 breaths/min with an inspiration/expiration ratio of 1/2 and 5 cm H_2O end-expiratory pressure (AV1, Dräger, Lübeck, Germany). The tidal volume (500–600 ml) was adjusted to maintain normal end-expiratory and arterial Pco_2. The pre-set ventilatory parameters were not modified during the experiment. P_ao_2, P_aco_2 and pH were measured by a blood gas analysis system (ABL 505, Blood Gas and Electrolyte System, Radiometer, Copenhagen, Denmark).

The left carotid artery and internal jugular vein were cannulated and the catheters were advanced into the aortic arch and the right atrium for monitoring arterial and central venous blood pressure, as well as for infusion and drug administration. A Swan-Ganz catheter was inserted into the left pulmonary artery via the right internal jugular vein to monitor pulmonary arterial pressure. Intravascular pressures were measured using Statham pressure transducers and registered on a multi-channel strip-chart recorder (Recomed 330, Hellige, Freiburg, Germany).

Lung injury was induced by a series of oleic acid (Merck, Darmstadt, FRG) injections into the left pulmonary artery through the distal opening of the Swan-Ganz catheter. The overall dose of oleic acid was 0.05 ml/kg body weight. Each injection contained an emulsion of 0.1 ml oleic acid and 0.9 ml warm electrolyte solution and was mixed well before administration. After each administration, the catheter was flushed with a warm electrolyte solution.

Experimental protocol

The experiments consisted of control measurements and measurements during the development of pulmonary injury. During the control phase EIT measurements, blood gas analysis and chest radiographs were obtained. Thereafter, oleic acid was injected sequentially at 12-min intervals until the full individual dose of oleic acid had been administered. In the time intervals between oleic acid injections, arterial blood samples were taken and EIT measurements performed. (The total number of measurements varied among the animals in the range of 19–25 as the number of oleic acid injections administered depended on individual body weight). Chest radiographs were obtained at hourly intervals.

After completion of the experiments, the animals were killed with potassium chloride injections and thoracotomies were performed. The lungs were removed and transverse slices of the left and right lower lung lobes, lying in the plane of EIT electrodes, were taken and cut into about 5 g samples. The lung tissue samples were weighed and dried in an oven at 100 °C for 24 h. Thereafter the wet to dry (W/D) weight ratio was calculated.

Application of EIT

The EIT device "Applied Potential Tomography System Mark I" (IBEES, Sheffield, UK) [7] was used in the experiments. Sixteen X-ray transparent electrodes (Blue Sensor BR-50-K, Medicotest A/S, Ølstykke, Denmark) were placed around the thorax in the form of a ring located about 3 cm below the axilla. Each pair of adjacent electrodes was sequentially used for electrical current (5 mA_{p-p}, 50 kHz) injection and the resulting potential differences were measured on the remaining adjacent electrode pairs. This rotating current injection and voltage detection is the basis for the calculation of regional intrathoracic impedance data from the registered surface potential differences with the Sheffield back-projection algorithm [8].

Immediately after each administration of oleic acid, separate EIT data acquisitions were performed and referred to as "EIT measurements". A schematic description of one EIT measurement is shown in Fig. 1. The standard EIT measurement consisted of two

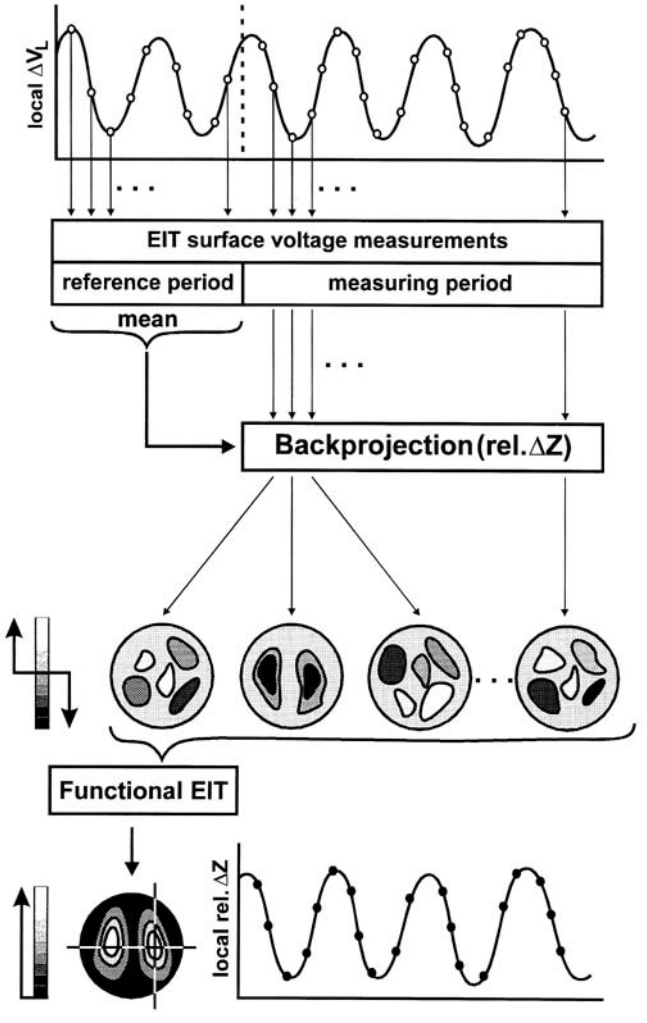

Fig. 1 Schematic EIT measurement. Surface voltage data resulting from electrical current injection are collected on the chest circumference during different phases of the respiratory cycle, i.e. at different intrathoracic lung volumes (V_L) (upper panel). One complete EIT measurement requires two separate impedance data collections: the reference and the measuring period. The mean surface voltage values are calculated from the data acquired during the reference period. All data collected subsequently during the measuring period are referred to the reference and provide a sequence of relative impedance change data (rel. ΔZ) reconstructed into a series of instantaneous simple EIT images using the back-projection algorithm. The number of EIT images corresponds with the number of data points collected during the measuring period. The EIT images represent the instantaneous change in impedance with respect to reference, therefore only images originating from data collection at lung volumes differing from the mean lung volume show lung-like structures (middle panel). The series of simple EIT images is processed by the functional EIT technique giving rise to one functional EIT image with clearly discernible lungs. The local time course of relative impedance change can be obtained in any image location (lower panel)

periods of 115 s and 240 s, respectively. The data acquired during the first sampling period were averaged and referred to as "reference". The data from the second sampling period ("measuring period") were processed by the back-projection algorithm, which calculated the normalised regional impedance changes. These values were referred to as "relative impedance changes". All regional relative impedance changes were given in a 32×32 matrix. Hence, the resultant circular image was composed of 912 pixels. Such images are the simple EIT images [2] and can be generated either in a grey or colour scale. In the current study, 240 black-and-white images were reconstructed from each 240 s long measurement, i.e. with an image sampling rate of 1 Hz.

Functional EIT imaging

All collected sets of simple EIT images were then processed by the new technique of functional EIT imaging [4]. One functional EIT image was generated from each series of 240 EIT images (Fig. 1). The principle of this procedure is shown in Fig. 2.

The functional EIT image is a cross-sectional representation of regional variation of relative impedance changes. The amount of local impedance variation was determined as the standard deviation of the time-dependent impedance changes in each image pixel position. Large impedance variation was represented in light tones and low variation in dark ones. To achieve a better visual effect, the image data were graphically interpolated by a factor of 4. The original functional EIT imaging software enabled additionally an interactive display of the time course of relative impedance change at any chosen cursor position. Using this approach, the original data entering the calculation of the impedance variation could be viewed and checked (Fig. 1, lower panels).

The effect of functional imaging can be described as follows. The impedance of the chest wall (ribs, backbone, muscles) does not change significantly in the course of the measurement, therefore the variation of local relative impedance change is low and these areas are imaged in dark tones. The impedance of the lungs varies largely with ventilation due to cyclical changes of air volume and, consequently, the lungs become visible as light areas (Fig. 2). Therefore, functional EIT tomograms are cross-sectional representations of regional ventilation and reflect its magnitude.

Evaluation of long-term regional ventilation changes

To display the isolated regional changes in ventilation magnitude associated with lung injury, "subtraction EIT images" were created. These images were generated by subtracting the functional EIT image obtained during control conditions from the functional EIT image acquired after lung injury development. Positive values in the subtraction image (dark tone) represent a regional increase in impedance variation due to locally augmented ventilation, and negative ones (light tone) its decrease (see lower panels in Fig. 4).

The development of regional ventilation changes was characterised by calculating the average impedance variation over the right and left lungs from the individual 19–25 measurements and plotted over time for each animal (see lower panels in Fig. 5). The region of the right and left lungs was defined as that area in the functional EIT image in which the variation of the relative impedance change was higher than 20% of the maximum standard deviation.

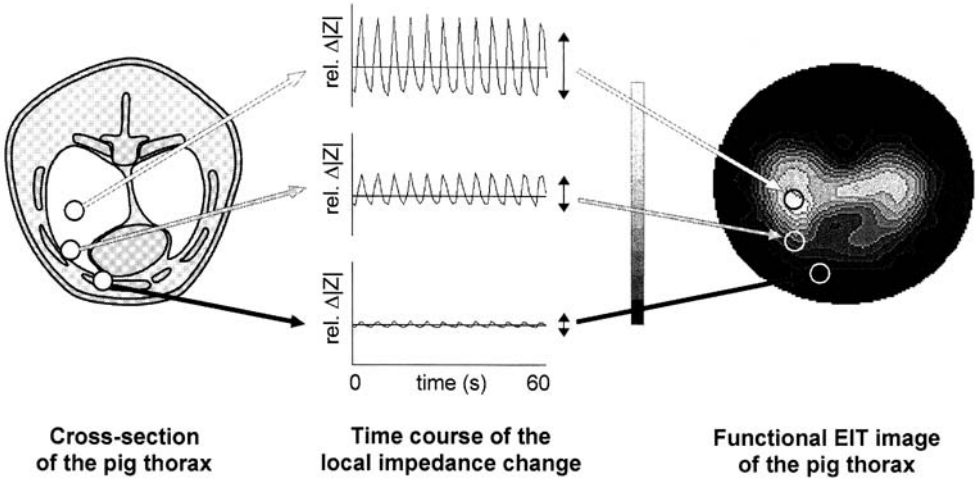

Fig. 2 Generation of a thoracic functional EIT image. The relative impedance change originating from the lungs varies largely with ventilation (upper time course of local impedance change), whereas only small variation of the measured relative impedance change is associated with other, non-pulmonary thoracic structures (lower time course of local impedance change). The local impedance variation is determined from the whole series of EIT images of instantaneous relative impedance change for each image pixel position, scaled and imaged in graded grey colour at the proper location giving rise to a functional EIT lung ventilation image (right). (The dorsal part of the thorax is at the top and the left side of the thorax on the right of the image.) Original data from a 60 s long EIT measurement in an anaesthetised mechanically ventilated pig with three individual time courses of the regional relative impedance change in single pixels and the resulting functional EIT image are shown

Evaluation of long-term changes in baseline impedance

To localise the long-term effect of oleic acid on the electrical properties of the lung tissue, images showing the shift in baseline impedance were generated. These images were created by the standard procedure for the generation of simple EIT images using the reference periods of the control measurement in combination with the reference periods from the subsequent measurements. The resulting 19–25 images of the change in baseline impedance were not affected by the short-term ventilation related impedance variations and display only the long-term shifts in baseline impedance distribution. The last image in each animal is shown in Fig. 4 (upper panels). Negative pixel values (light tone) imply a local decrease of impedance e.g. due to lung water accumulation.

To reflect the trend during the whole experiment, the baseline impedance data were averaged over the right and left lungs in all measurements and presented graphically as a function of time for each animal (see middle panels in Fig. 5). The area of the right and left lungs was defined according to the same criteria as stated above.

The results obtained during the control conditions and the last measurement are given in the text as mean values ± SD. The Student's *t*-test was used to test the significance of differences between the controls and the last data for the five animals studied. A p value less than 0.05 was considered significant.

Results

Electrical impedance tomography (EIT)

Affected left lung

In all animals the impedance variation was reduced over the affected lung compared with the respective control (Fig. 3). This was also clearly shown by the subtraction images (Fig. 4, lower panels). The continuous fall of the impedance variation averaged over the left lung during the experiment is shown in Fig. 5 (lower panels). The impedance variation was reduced by 41.4 ± 8.2% (mean ± SD) by the end of the measuring period.

A pronounced fall in baseline impedance was observed over the affected lung (Fig. 4, upper panels). The continuous shift of lung impedance was evidenced by the time course of baseline impedance averaged over the left lung reaching –20.6 ± 1.9% by the end of the experiment when compared with control (Fig. 5, middle panels).

Unaffected right lung

The impedance variation was increased in the unaffected lung, which is in contrast to the affected one. The images in Fig. 3 (lower panels), the subtraction images in Fig. 4 (lower panels) and the time course of the impedance variation averaged over the right lung (Fig. 5, lower panels) show this finding. The impedance variation averaged over the right lung rose by 20.4 ± 14.2% (mean ± SD) by the end of the experiment when compared with control.

Similarly to the affected lung, a long-term decrease of electrical impedance was observed in the unaffected one (Fig. 4, upper panels; Fig. 5, middle panels). The fall in baseline impedance was less pronounced than in

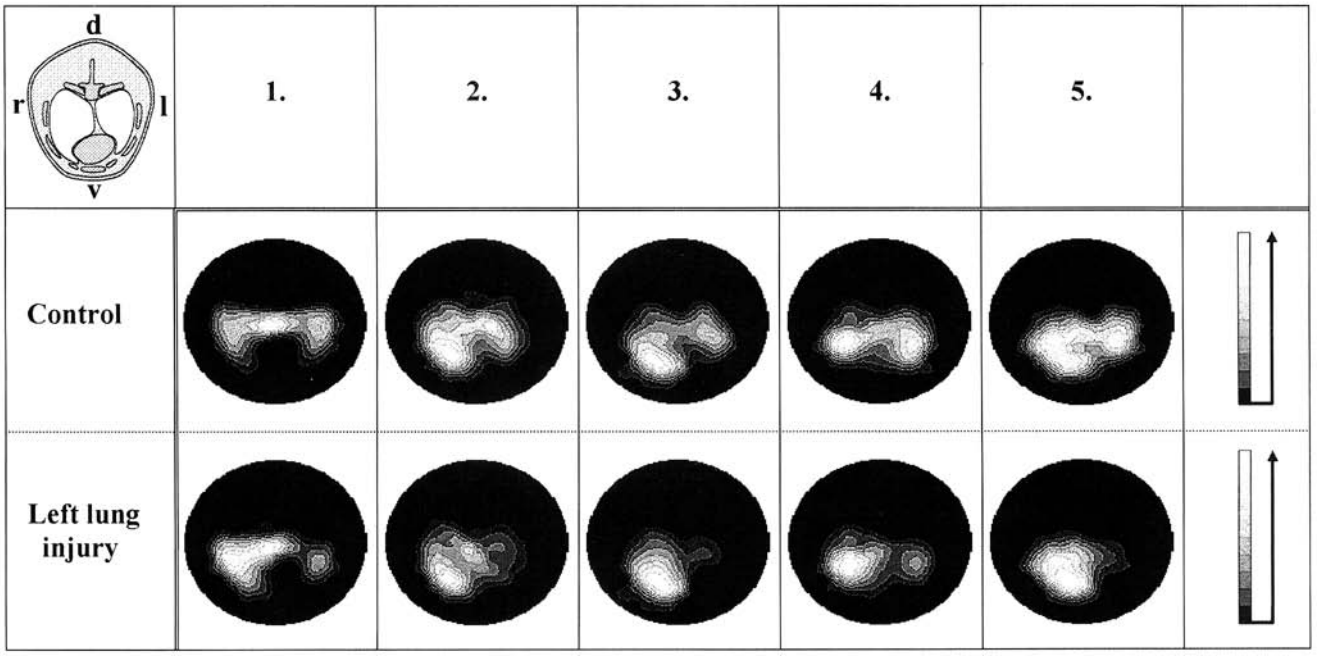

Fig. 3 Thoracic functional EIT images before (Control) and after the development of artificially induced left lung injury (Lung injury) reflecting the distribution of ventilation in the five animals studied. (The lungs are typically located in the central and ventral parts of the thorax due to the well developed backbone musculature in pigs.) The schematic cross-section of the pig thorax in the left upper corner shows the spatial orientation of the images. Each image is scaled to the individual maximum impedance variation. The scale shows that higher local impedance variation (i.e. higher fluctuation of regional lung volume) is represented in light tones

Table 1 Parameters of acid base balance and pulmonary arterial pressure (mean values ± SD) during control measurements and during fully developed unilateral lung injury artificially in ventilated pigs ($n = 5$). (P_aCO_2 carbon dioxide arterial partial pressure, P_aO_2 oxygen arterial partial pressure, *Pap* mean pulmonary arterial pressure)

	Control	Lung injury
$PaCO_2$ (mm Hg)	37.1 ± 2.5	40.1 ± 4.0*
PaO_2 (mm Hg)	187.5 ± 18.1	112.3 ± 46.0*
pH	7.42 ± 0.06	7.35 ± 0.09*
Pap (mm Hg)	20.8 ± 2.9	29.2 ± 4.2*

* $p < 0.05$

the injured lung and reached –10.0 ± 4.4 % by the end of the measuring period.

Blood gas analysis

The administration of oleic acid resulted in acute respiratory distress with increased pulmonary arterial pressure, affected arterial blood gas tensions and progressive development of respiratory acidosis (Table 1). The individual time courses of P_ao_2 and P_aco_2 during the experiments, related to the time courses of the EIT parameters, are shown in Fig. 5 (upper panels).

Morphological reference techniques

The occurrence of unilateral acute lung injury was documented by chest X-rays with hazy and less radiolucent left lung in each animal. The post-mortem inspection of the lungs revealed dark red haemorrhages on the surface of the left lung. The injured lung was stiff, filled with fluid and pleural exudate was found in the interpleural space. No such macroscopical changes were found in the untreated lung. The evaluation of the lung tissue samples from the lung treated with oleic acid and from the non-affected lung, analysed in terms of the W/D weight ratio, proved the predominant occurrence of oedema in the left lung ($p < 0.01$). The mean W/D weight ratio ± SD in the left and right lungs was 8.83 ± 0.94 and 6.90 ± 0.48, respectively. No significant difference between the W/D weight ratios from the ventral and dorsal regions was found in the affected lung (8.70 ± 0.82 vs 8.64 ± 1.94) whereas significant differences were determined in the unaffected lung (6.73 ± 0.41 vs 7.11 ± 0.46).

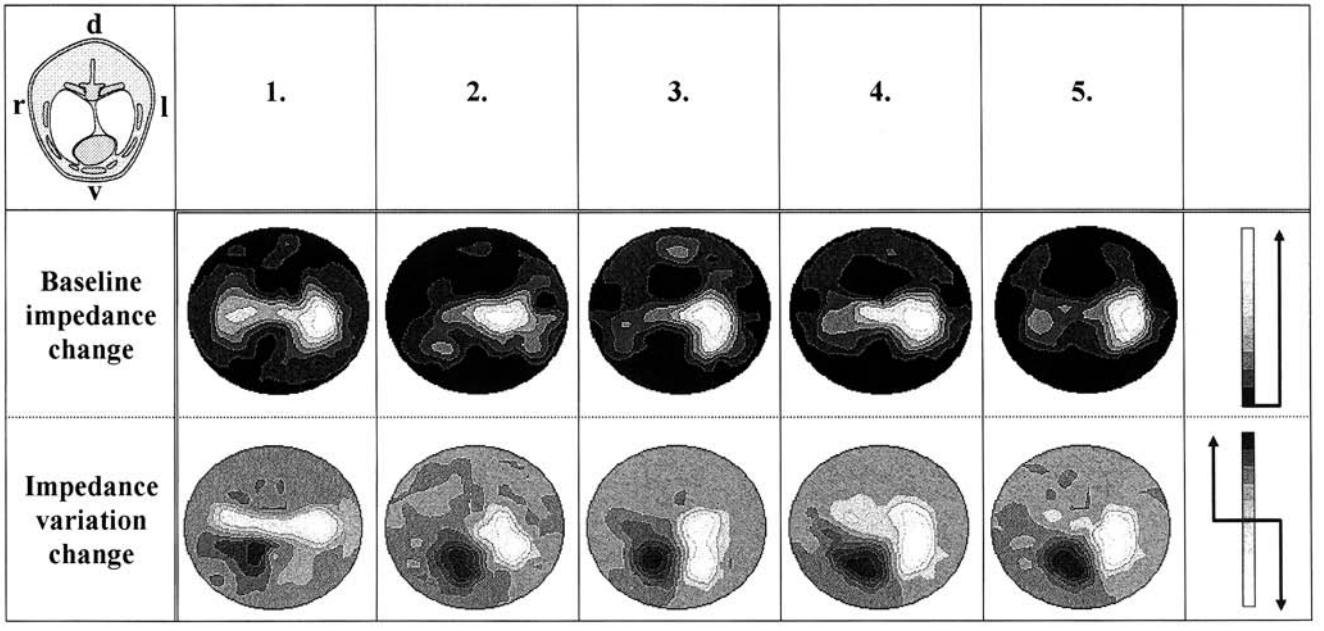

Fig. 4 EIT images of long-term shift in baseline impedance between control conditions and the state of left lung injury showing the pronounced fall in left lung tissue impedance (upper panels) and subtraction images showing the increased and decreased ventilation of the right and left lung respectively (lower panels). The order of the EIT tomograms corresponds with that of the functional EIT images in Fig. 3. The *upper right-hand scale* shows that a decrease in baseline impedance is depicted in light tones. The *lower right-hand scale* indicates that a decrease in regional ventilation magnitude manifests itself in light tones and an increase in dark ones

Discussion

Model of lung injury

Intravenous administration of oleic acid is a well established method of inducing acute respiratory distress [9–12]. In view of the goal of our study, it was necessary to induce lung injury in a protracted way. Therefore, oleic acid was administered in a series of injections [12, 13]. The overall dose of oleic acid used was comparable with other studies in pigs. The pulmonary injury induced exhibited all the typical characteristics of acute lung damage. The findings of pulmonary vascular hypertension and impaired gas exchange corresponded to the observations of other authors [9–12]. The chest radiographs and the post-mortem changes with significantly higher W/D weight ratio in the affected lung confirmed the presence of injury in the left lung.

The unilateral lung injury model was chosen as the unaffected lung provided an "internal reference" for the simultaneously observed changes in the injured lung. This is a substantial difference to other EIT studies on lung oedema, where global lung injury was induced [14, 15]. This model enabled us to study the complex pattern of changes of the pulmonary function (e.g. the redistribution of ventilation in response to the local degree of oedema formation).

EIT measurements

Already in the early studies on EIT, it was suggested that this technique might be useful in monitoring pulmonary disorders [16, 17]. The first attempts at implementing simple EIT in respiratory applications were encouraged by the theoretical analysis of impedance imaging [8]. A linear relationship between the changes of lung volume and measured impedance [16, 18], as well as an overall correspondence between spirometric and EIT recordings were determined [4, 16]. The few follow-up "respiratory" applications of EIT focused on the morphological information (e.g. identification of extremely large bullae [19]) and were partly performed during deep ventilatory manoeuvres [20, 21]. Only such extreme manoeuvres producing large impedance changes guaranteed the generation of useable EIT images. The quality of the EIT images in all these applications was very low when compared with established medical imaging techniques.

The functional EIT technique [4] is different from the "morphological" approach in simple EIT. It was introduced with the aim of obtaining and imaging functional information from EIT measurements during tidal breathing or artificial ventilation, i.e. under such ventilatory conditions as are relevant in clinical settings. Extreme manoeuvres are not acceptable, as they are po-

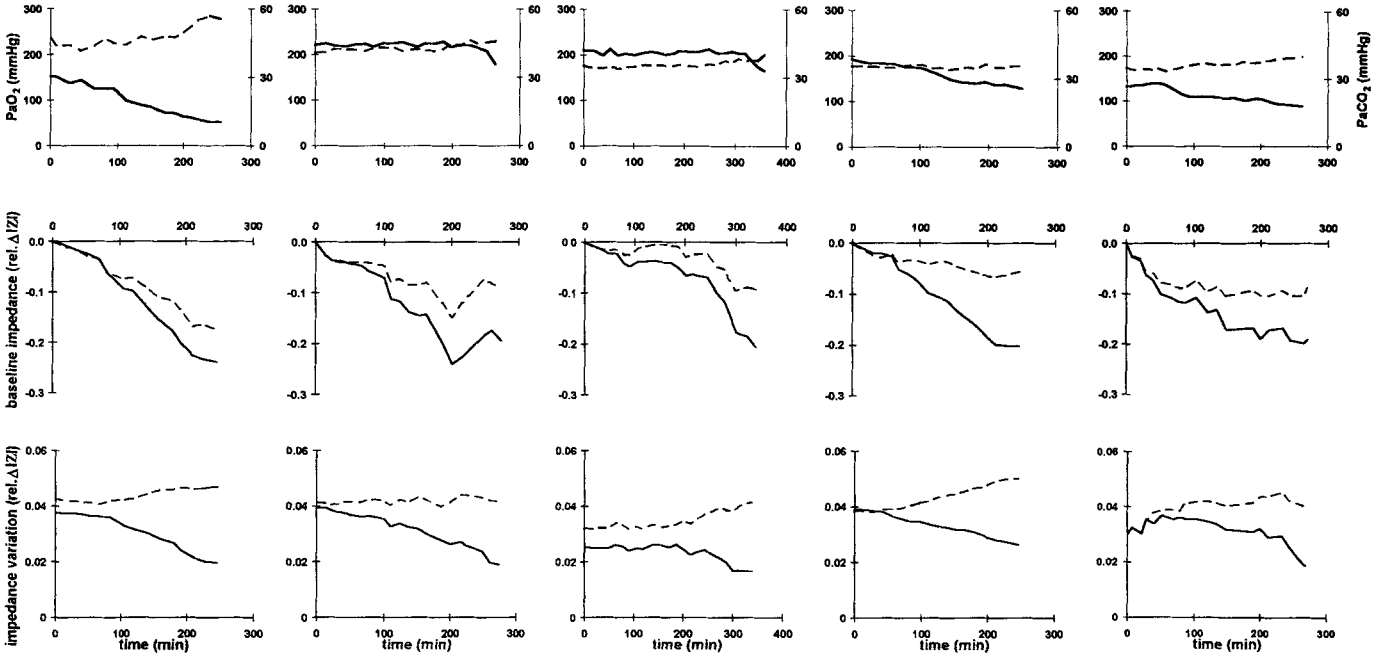

Fig. 5 The time courses of 1) P_aO_2 (solid line) and P_aco_2 (dashed line) (upper panels), 2) the baseline impedance shift over the left (solid line) and right lung (dashed line), referred to control (middle panels) and 3) the impedance variation in the left (solid line) and right lung (dashed line) (lower panels) of individual animals. The order of the panels corresponds with that of the EIT tomograms in Figs. 3 and 4

tentially dangerous (e.g. barotrauma) and may interfere with the clinical situation. Functional EIT offered the possibility to collect large sets of EIT data based on a small magnitude of relative impedance changes and to process them statistically. The long data collection period made possible the calculation of functional images from a higher number of single images and resulted in a marked improvement of the image quality. Using simple EIT, only a limited number of single images with significant stochastic instability could be acquired during the short duration of the ventilatory manoeuvres (e.g. 5 s [20]).

In the current study, an experimental lung injury was followed by functional EIT. In general, lung injury alters the mechanical properties of the affected lung and leads to a redistribution of ventilation in favour of the intact lung. The expected changes in regional magnitude of ventilation were reflected by changes in regional impedance variation in all animals. Impedance variation over the injured lung decreased in accordance with the reduction of properly ventilated lung tissue whereas that of the contralateral lung increased, which corresponds with higher local tidal volume associated with constant ventilator settings. This inverse behaviour of the affected and unaffected lung was detected by the primary functional EIT tomograms (Fig. 3), the subtraction images (Fig. 4, lower panels) and the individual time courses (Fig. 5, lower panels) of the impedance variation over the left and right lungs.

The accumulation of extravascular fluid in the lungs with the formation of interstitial or intra-alveolar lung oedema is the other typical component in the pathology of lung injury. The EIT images and the individual time courses, showing the long-term shift in regional baseline impedance (Fig. 4, upper panels and Fig. 5, middle panels), reflected this effect as a pronounced decrease of impedance in the affected lung. However, a less significant fall of regional impedance was detected in the intact lung as well. This phenomenon may be explained by the development of atelectasis in the dependent parts of the lungs, which is known to occur during prolonged mechanical ventilation, [22] or with oedema, which may develop even during unilateral oleic acid administration [23]. Both atelectasis and lung injury manifest themselves by a decrease of impedance. At present, pathogenetically dissimilar processes associated with a general decrease of impedance (e.g. fluid and blood accumulation, atelectasis, reduction of residual air volume) cannot be differentiated. It remains to be clarified whether the application of injection currents with differing frequencies will add this feature to functional EIT. However, the interpretation of multi-frequency measurements [24, 25] with respect to the underlying pathophysiological mechanisms is not yet satisfactory [14].

The decline in impedance variation and baseline impedance over the affected lung occurred in the same parts of the subtraction images and the images of base-

line impedance shift. Over the unaffected lung, a more ventrally located increase in impedance variation and dorsally indicated fall in baseline impedance were observed. This may reflect a) the homogeneity of lung damage in the left lung with accumulation of lung water and reduction of ventilation in the whole affected tissue and b) the better ventilation of the non-dependent lung regions and atelectasis or oedema in the dependent parts of the right lung. The EIT results were confirmed by the regional W/D weight ratios, that exhibited significant differences between the dependent and non-dependent regions in the unaffected lung but no differences in the injured lung.

An interesting phenomenon is that, in two of the animals studied, EIT provided early information on changes of the lung function. In animals 2 and 3 constant P_aO_2 and P_aCO_2 were found during almost the whole experiment in spite of changes detected in chest X-rays and in the time courses of baseline impedance and impedance variation (Fig. 4, 2nd and 3rd column of panels). The ability of EIT to indicate an early development of lung injury may be related to the complex histological changes resulting from oleic acid administration, which are known to vary from mild and focal to severe and diffuse [12]. The gas exchange was not severely compromised at the beginning of lung injury, but the electrical conductivity of the affected tissue rose continuously and, therefore, was identified by EIT.

In conclusion, the current study has shown that a long-term disturbance of the lung function can be followed by functional EIT. Both the development of the unilateral lung injury and the accompanying ventilation redistribution in the lungs was monitored over a period of several hours. These results indicate the future possibility of applying functional EIT in non-invasive bedside monitoring of regional lung function in the clinical environment. This technique may become useful in assessing the progression of such pathological changes that are associated either with shifts in baseline impedance or in impedance variation. However, clinical acceptance of this technique will depend on the future development of the EIT hardware and software.

References

1. Geddes LA, Baker LE (1967) The specific resistance of biological material – a compendium of data for the biomedical engineer and physiologist. Med Biol Eng J 5: 271–293
2. Barber DC, Brown BH (1984) Applied potential tomography. J Phys E: Sci Instrum 17: 723–733
3. Cheney M, Isaacson D, Newell JC, Simske S, Goble J (1990) NOSER: An algorithm for solving the inverse conductivity problem. Int J Imag Syst Technol 2: 66–75
4. Hahn G, Šipinková I, Baisch F, Hellige G (1995) Changes in the thoracic impedance distribution under different ventilatory conditions. Physiol Meas 16:A161–A173
5. Kaneko K, Milic-Emili J, Dolovich MB, Dawson A, Bates DV (1966) Regional distribution of ventilation and perfusion as a function of body position. J Appl Physiol 21: 767–777
6. Frerichs I, Hahn G, Hellige G (1996) Gravity-dependent phenomena in lung ventilation determined by functional EIT. Physiol Meas 17:A149–A157
7. Brown BH, Seagar AD (1987) The Sheffield data collection system. Clin Phys Physiol Meas 8(Suppl A):91–97
8. Barber DC (1990) Quantification in impedance imaging. Clin Phys Physiol Meas 11 (Suppl A):45–56
9. Zetterström H, Jakobson S, Janerås L (1981) Influence of plasma oncotic pressure on lung water accumulation and gas exchange after experimental lung injury in the pig. Acta Anaesth Scand 25: 117–124
10. Kruse-Elliott K, Olson NC (1990) Role of leukotrienes during oleic acid-induced lung injury in pigs. J Appl Physiol 68: 1360–1367
11. Haldén E, Hedstrand U, Torsner K (1982) Oleic acid lung damage in pigs. Acta Anaesth Scand 26: 121–125
12. Grotjohan HP, van der Heijde RMJH (1992) Experimental Models of the Respiratory Distress Syndrome Lavage and Oleic Acid. Erasmus University, Rotterdam, pp 1–239
13. Böck JC, Hoeft A, Korb H, Hellige G (1989) Characteristics of the pulmonary transport functions for heart and dye in pulmonary oedema and orthostasis. Biomed Tech 34: 85–90
14. Brown BH, Flewelling R, Griffiths H, Harris ND, Leathard AD, Lu L, Morice AH, Neufeld GR, Nopp P, Wang W (1996) EITS changes following oleic acid induced lung water. Physiol Meas 17:A117–A130
15. Newell JC, Edic PM, Ren X, Larson-Wiseman JL, Danylecko MD (1996) Assessment of acute pulmonary edema in dogs by electrical impedance imaging. IEEE Trans Biomed Eng 43: 133–139
16. Harris ND, Suggett AJ, Barber DC, Brown BH (1987) Applications of applied potential tomography (APT) in respiratory medicine. Clin Phys Physiol Meas 8 (Suppl A):155–165
17. Brown BH, Barber DC, Seagar AD (1985) Applied potential tomography: possible clinical applications. Clin Phys Physiol Meas 6: 109–121
18. Harris ND, Suggett AJ, Barber DC, Brown BH (1988) Applied potential tomography: a new technique for monitoring pulmonary function. Clin Phys Physiol Meas 9 (Suppl A):79–85
19. Eyuboglu BM, Oner AF, Baysal U, Biber C, Keyf AI, Yilmaz U, Erdogan Y (1995) Application of electrical impedance tomography in diagnosis of emphysema – a clinical study. Physiol Meas 16:A191–211
20. Holder DS, Temple AJ (1993) Effectiveness of the Sheffield EIT system in distinguishing patients with pulmonary pathology from a series of normal subjects. In: Holder D (ed) Clinical and Physiological Applications of Electrical Impedance Tomography. UCL Press, London, pp 277–298
21. Brown BH, Barber DC (1987) Electrical impedance tomography; the construction and application to physiological measurement of electrical impedance images. Med Prog Technol 13: 69–75
22. Tokics L, Hedenstierna G, Strandberg A, Brismar B, Lundquist H (1987) Lung collapse and gas exchange during general anesthesia: effects of spontaneous breathing, muscle paralysis and positive end-expiratory pressure. Anesthesiology 66: 157–167
23. Fredén F, Cigarini I, Mannting F, Hagberg Å, Lemaire F, Hedenstierna G (1993) Dependence of shunt on cardiac output in unilobar oleic acid edema. Distribution of ventilation and perfusion. Intensive Care Med 19: 185–190
24. Brown BH, Barber DC, Leathard AD, Lu L, Wang W, Smallwood RH (1994) High frequency EIT data collection and parametric imaging. Innov Tech Biol Med 15: 1–8
25. Osypka M, Gersing E, Meyer-Waarden K (1993) Komplexe elektrische Impedanztomographie im Frequenzbereich von 10 Hz bis 50 kHz. Z Med Phys 3: 124–132